Different Populations of Tyrosine-hydroxylase-immunoreactive Neurons Defined by Differential Expression of Nitric Oxide Synthase in the Human Temporal Cortex

Ruth Benavides-Piccione and Javier DeFelipe

Instituto Cajal (CSIC), Madrid, Spain

In the mammalian neocortex, neurons containing tyrosine hydroxylase (TH), the rate-limiting enzyme in catecholamine synthesis, constitute an enigmatic and ill-defined group of aspiny non-pyramidal cells. In the human neocortex, these neurons are mostly found in layers V–VI, the same layers in which another conspicuous group of nitrergic non-pyramidal cells are found — those containing nitric oxide synthase (nNOS) and that can be labeled by nicotinamide adenine dinucleotide phosphate diaphorase (NADPHd) histochemistry. The main aim of the present study was to determine the extent to which neurons and fibers containing TH, NADPHd or nNOS co-localize in the human temporal cortex, using immunocytochemistry and NADPHd histochemistry. Furthermore, we have quantified the degree to which axons immunoreactive (ir) for TH contact the somata of neurons by co-labeling with the neuron-specific nuclear protein NeuN. As a result, we show that the population of TH-ir neurons can be subdivided into two main neurochemical groups: those expressing nNOS (26%) and those that do not (74%). There was no co-localization of TH with nNOS in the prominent horizontally oriented plexus of fibers in layer I and we did not observe any double bouquet cells, chandelier cells or basket cells that contained TH. Finally, we observed that only 6% of the TH-ir axonal boutons examined ($n = 1724$) could be seen to contact neuronal somata. Thus, most TH-ir axons must form synapses with dendrites. In conjunction with data from previous studies, these results suggest that TH is found in different neurochemically defined subpopulations of non-pyramidal neurons in layers V–VI of the human temporal cortex. Consequently, it appears that a partial overlap of the catecholaminergic and nitrergic systems is probably due to the intrinsic cortical TH-nNOS-ir neurons.

Introduction

Catecholamines have been shown to be involved in a variety of processes and pathologies such as Alzheimer's disease and schizophrenia (Palmer, 1996; Goldman-Rakic, 1998; Lidow *et al.*, 1998; Lewis and Lieberman, 2000). Whilst catecholaminergic fibers are widely distributed throughout the nervous system, catecholaminergic neurons are restricted to certain regions of the brain and spinal cord, including the cerebral cortex (Smeets and González, 2000). In the neocortex, neurons that are immunoreactive (ir) for tyrosine hydroxylase (TH), the rate-limiting catecholamine synthesizing enzyme, constitute an enigmatic and ill-defined group of aspiny non-pyramidal cells. The laminar distribution of these neurons is markedly different across species, as is the co-expression of GABA (or GAD). For example, in the neocortex of certain cetaceans, TH-ir neurons are mainly confined to layer I (Hof *et al.*, 1995), whereas in the rat, TH-ir neurons are found in all the cortical layers, although they are most abundant in layers II–III. In addition, the majority of TH-ir neurons in the rat cortex co-express GABA or GAD (Kosaka *et al.*, 1987a). In the human neocortex, TH-ir neurons are found mostly in layers V–VI, although only 50% contain GABA (Gaspar *et al.*, 1987; Hornung *et al.*, 1989; Kuljis *et al.*, 1989; Trottier *et al.*, 1989). This observation is striking because it is thought that most non-pyramidal neurons are GABAergic and thus inhibitory (Houser *et al.*, 1984). In spite of these peculiarities and their possible involvement in CNS diseases, the lack of information regarding cortical TH neurons is remarkable, in particular with respect to the human neocortex.

In the human cortex, apart from the population of TH-ir neurons, another group of non-pyramidal cells is particularly conspicuous in layers V–VI and these cells can be labeled by nicotinamide adenine dinucleotide phosphate diaphorase (NADPHd) histochemistry (Unger and Lange, 1992; Akbarian *et al.*, 1993; DeFelipe, 1993). The morphology of these NADPHd-positive neurons and fibers is similar to those labeled for TH. Furthermore, it has been shown that neuronal nitric oxide synthase (nNOS), a Ca^{2+}/calmodulin-dependent enzyme required for the synthesis of nitric oxide in neurons, frequently co-localizes with NADPHd (Bredt *et al.*, 1991; Dawson *et al.*, 1991; Huang *et al.*, 1993). Indeed, a wide variety of neurotransmitters, neuropeptides and calcium-binding proteins has been found in neurons expressing nNOS, including GABA, calbindin, somatostatin and neuropeptide Y (Unger and Lange, 1992; Valtschanoff *et al.*, 1993; Hashikawa *et al.*, 1994; Kubota *et al.*, 1994; Bertini *et al.*, 1996; Yan *et al.*, 1996; Gonchar and Burkhalter, 1997; Estrada and DeFelipe, 1998; González-Albo *et al.*, 2001). Thus, this group of nitrergic non-pyramidal cells can be characterized by the expression of multiple neuronal markers with a variety of functions.

The main goal of the present work was to determine to what extent neurons and fibers containing TH and NADPHd/nNOS overlap in the human temporal cortex, by using single- and double-labeling immunocytochemistry and histochemistry. Furthermore, we have quantified the degree to which TH-ir axons contact the somata of neurons by co-labeling with the neuron-specific nuclear protein NeuN.

Materials and Methods

Human tissue from two sources was used: post-operative tissue (Department of Neurosurgery, Hospital de la Princesa, Madrid, Spain) and tissue from autopsies (kindly supplied by Dr R. Alcaraz, Forensic Pathology Service, Basque Institute of Legal Medicine, Bilbao, Spain). Post-operative human tissue was obtained from three male patients (H39, H57 and H59, aged 25, 27 and 30 years, respectively) suffering pharmacoresistant right temporal lobe epilepsy (partial complex with secondary generalized tonic–clonic seizures). Tissue specimens were taken from biopsies collected for neuropathological assessment. Informed consent was obtained from each patient prior to surgery. The neocortical tissue was considered to be normal on the basis of electrophysiological and histopathological examination. Indeed, some of this material was also used in an earlier study in which the authors detailed the clinical information and the criteria followed to establish that the resected tissue was normal (González-Albo *et al.*, 2001). Human tissue obtained at autopsy (2–3 h *post mortem*) was from two normal males (aged 23 and 49 years) that died in traffic accidents. All portions of neocortex used

were from the right anterolateral inferior temporal gyri – Brodmann's area 20 (Garey, 1994).

Tissue Preparation

Surgically resected tissue was immediately immersed in cold 4% paraformaldehyde in 0.1 M phosphate buffer (PB), pH 7.4. After 2–3 h, the tissue was cut into small blocks (~15 × 8 × 8 mm) and postfixed in the same fixative for 24 h at 4°C. The brain tissue from autopsies was sectioned into 1.5 cm thick coronal slices and fixed by immersion in cold 4% paraformaldehyde in PB. Small blocks of cortex were then transferred to a second solution of 4% paraformaldehyde in PB for 24 h at 4°C. Thereafter, all tissue blocks were cryoprotected in 25% sucrose in PB and stored at –20°C in a solution of glycerol, ethylene glycol and PB. Vibratome sections (100 μm) of the tissue were obtained and pretreated with a solution of ethanol and hydrogen peroxide in PB to remove endogenous peroxidase activity. Some of the sections were processed for NADPHd histochemistry and for immunoperoxidase procedures, whereas others were processed for double immunocytochemical staining. Adjacent sections were stained with thionine.

NADPHd Histochemistry

Sections were processed for NADPHd histochemistry according to a published protocol (Hope and Vincent, 1989). Briefly, sections were washed in 50 mM Tris–HCl, pH 7.4 and incubated for 60 min at 37°C in 1 mM β-NADPH (Sigma, St Louis, MO), 0.5 mM nitroblue tetrazolium (NBT; Sigma) and 0.1% Triton X-100 in 50 mM Tris–HCl, pH 8. The sections were then rinsed in 50 mM Tris–HCl, pH 7.4 and washed in PB. The sections were mounted, dehydrated, cleared in xylene and then coverslipped.

Immunocytochemistry

Single-labeling Procedure

Sections were preincubated in 3% normal serum (horse or goat) in PB with Triton X-100 (0.25%) for 2 h at room temperature. Sections were then incubated for 24 h at 4°C in the same solution containing either mouse anti-tyrosine hydroxylase (1:1000; Diasorin, Stillwater, MN) or rabbit anti-nNOS (1:250; Chemicon, Temecula, CA). The sections were subsequently washed in PB and incubated for 1 h at room temperature in biotinylated goat anti-rabbit IgG or horse anti-mouse diluted 1:200 in PB (Vector, Burlingame, California). The sections were then processed using the Vectastain ABC immunoperoxidase kit (Vector) and the antibody distribution detected histochemically with 0.05% 3,3'-diaminobenzidine tetrahydrochloride (DAB; Sigma) and 0.01% hydrogen peroxide. The sections were finally mounted, dehydrated, cleared with xylene and coverslipped.

Double-labeling Procedure

Two methods were used for double immunocytochemical staining: that involving conventional light microscopy and a second method to analyze the material by fluorescence and confocal laser microscopy.

Conventional light microscopy for TH and NeuN. Sections were sequentially processed for TH and NeuN immunocytochemistry. This latter antibody (Chemicon) is a specific marker for neurons that recognizes a neuron-specific, soluble, nuclear, DNA-binding protein in vertebrates. It is present in the nucleus and perikarya, including proximal dendritic processes, of the vast majority of mature neuronal cells in both the central and peripheral nervous systems of different vertebrate species, including humans (Mullen *et al*., 1992; Wolf *et al*., 1996; Sarnat *et al*, 1998). Sections were first stained for TH using the same mouse monoclonal antibody and dilutions as indicated above. The sections were then washed and reprocessed for mouse anti-NeuN staining (1:2000) using the same single-labeling immunocytochemical procedure.

Confocal laser microscopy for TH and nNOS. Sections were double-stained for TH and nNOS using the same mouse monoclonal and rabbit polyclonal antibodies and dilutions indicated above. Following incubation in the primary antibodies, sections were washed in PB and incubated for 1 h at room temperature in biotinylated horse anti-mouse IgG diluted to 1:200 in PB (Vector). Sections were then washed in PB and incubated for 2 h at room temperature in a mixture of Alexa-fluor-594-conjugated goat anti-rabbit (1.1000) and Alexa-fluor-488-conjugated streptavidin (1:1000; Molecular Probes, Eugene, OR). In all cases, sections were processed as a single batch. Finally, sections were mounted in 50% glycerol in PB.

Control sections were processed as above; however, the primary antibody was omitted or, alternatively, the secondary antibody was replaced with an inappropriate secondary antibody. No specific labeling was observed under these control conditions. Double-labeled sections were studied with the aid of a Leica TCS 4D confocal laser scanning microscope equipped with an argon/krypton mixed gas laser and a Leitz DMIRB fluorescence microscope. Fluorescent-labeled profiles were imaged through separate channels. Excitation peaks of 585 and 491 nm were used to visualize Alexa fluor 594 and 488, respectively.

Quantitative Analyses

To measure cell size (surface area, perimeter and major and minor axes), we used sections immunostained for TH (using DAB as the chromagen) and sections prepared for NADPHd histochemistry. These techniques provided us with optimal material in terms of morphology and labeling. In material that was processed for immunofluorescence, dendrites were labeled in relatively few cells. A total of 60, randomly selected, clearly labeled, morphologically and neurochemically characterized neurons (10 per type of TH-ir bipolar, TH-ir tripolar, TH-ir multipolar, NADPHd bipolar, NADPHd tripolar and NADPHd multipolar) were measured in layers V–VI. The somatic profiles of neurons labeled for TH and NADPHd were traced with a drawing tube fixed to the microscope using a ×100 objective lens (final magnification ×1640) and printed. These drawings were then measured using a magnetic tablet (SummaSketch III) and the Scion Image image analysis program (Scion Corp., Frederick, MD).

To estimate the degree of co-localization between TH and nNOS in layers V–VI, double-labeled sections were studied with the aid of an Olympus BX50WI microscope equipped with a mercury fluorescence light source and using a ×40 objective (188 500 μm^2 field). For this purpose, we first counted TH-ir neurons in each field and then, by switching filters to visualize nNOS, single- and double-labeled neurons were recorded. A total of 430 fields were analyzed from two biopsies (190 in case H39 and 240 in case H57). In these fields, 276 TH-ir neurons (114 and 162, respectively) and 375 nNOS-ir neurons (129 and 246, respectively) were sampled.

For quantitative estimates of the numbers of TH-ir fibers (axonal boutons) in contact with somata of neurons (appositions), sections double labeled for TH and NeuN, were examined with the aid of a microscope equipped with a Hitachi CCD color video camera. Images were captured using a computer at a final magnification of ×3000 using a ×100 objective lens and printed. These images were captured at a single focal depth in the superficial portion of the section to which both primary antibodies had penetrated.

A total of 74 rectangles (62 × 47 μm) were sampled in images from layer II or layer VI from the three surgically resected cortical tissue biopsies (38 rectangles in H39; 18 in H57; 18 in H59). Each NeuN-ir soma (including fragments of cell bodies) and all the TH-ir axons in the same focal plane were counted. In this manner, a total of 1724 TH-ir axons (746 in H39; 392 in H57; 586 in H59) and 163 NeuN-ir neurons (90 in H39; 37 in H57; 36 in H59) were examined. The data were expressed collectively as the percentage of TH-ir boutons in contact with NeuN-ir somata, the percentage of NeuN-ir neurons showing such contacts and the percentage of TH-ir axonal boutons in the neuropil. Axonal boutons were considered to be in contact with a soma when both labeled elements appeared to be in direct apposition in the same focal depth and there was no apparent space between them.

Results

We have compared the distribution of TH, nNOS and NADPHd in human cortical tissue obtained from five male subjects. No differences could be detected between the patterns of immunohistochemical labeling in cortical tissue from autopsy or from surgically resected cases. However, the density of labeled fibers and neurons was higher and with better morphology in the tissue obtained by surgery. Therefore, we will refer only to surgically resected tissue, unless otherwise stated.

Morphology and Distribution of TH-ir, nNOS-ir and NADPHd-positive Neurons

In the neocortex, TH-ir neurons displayed a non-pyramidal morphology and were restricted almost exclusively to layers V–VI (Fig. 1*A*,*D*). A variety of shapes and sizes were observed (ranging from 96 to 208 μm^2 in area; Table 1), although the most common morphology was that of a bipolar and bitufted shape with vertically oriented dendrites (Fig. 2*C*,*D*). These cells constituted 63% of the total population of TH-ir neurons analyzed (n = 584). The majority of the remaining TH-ir neurons were either tripolar (19%), or multipolar (12%; Fig. 4).

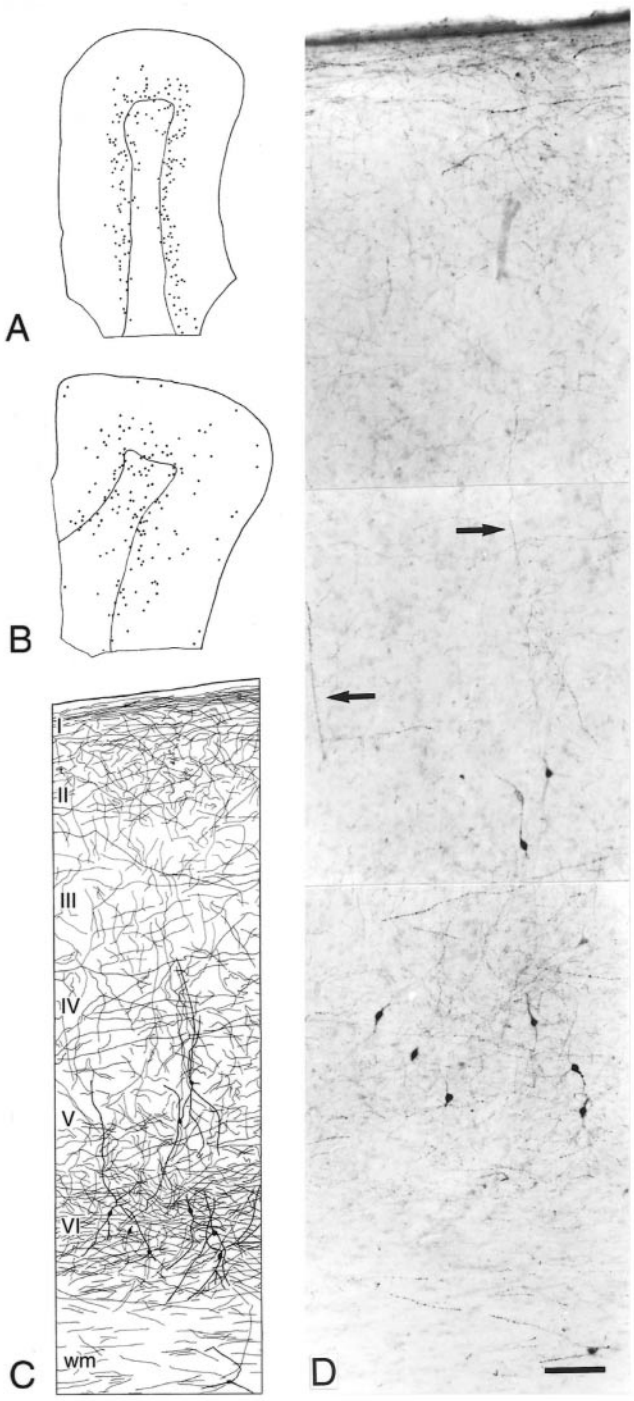

Figure 1. Camera lucida drawings of TH-ir (*A*) and NADPHd stained (*B*) neurons in area T3 (Brodmann's area 20) of the human temporal cortex. (*C*) Camera lucida drawing showing the laminar distribution of TH-ir neurons and fibers. (*D*) Photomicrograph of the section in (*C*), showing TH-ir neurons and fibers throughout layer I to the white matter. Notice the labeling of neurons in layers V–VI. Arrows indicate vertically oriented fibers. Scale bars = 2 mm (*A*, *B*), 220 μm (*C*) and 120 μm (*D*).

Table 1
Cell size measurements (mean ± SD) of different morphological types of TH-ir and NADPHd-positive neurons

Morphological type	Surface area (μm^2)	Perimeter (μm)	Major axis (μm)	Minor axis (μm)
TH-ir bipolar	161 ± 37*	52 ± 7**	19 ± 2**	10 ± 2
TH-ir tripolar	149 ± 28**	52 ± 6**	17 ± 2**	11 ± 2
TH-ir multipolar	162 ± 29*	52 ± 6*	18 ± 4	11 ± 2
NADPHd-positive bipolar	220 ± 54	65 ± 8	25 ± 4	11 ± 3
NADPHd-positive tripolar	211 ± 43	61 ± 6	22 ± 3	12 ± 2
NADPHd-positive multipolar	220 ± 80	60 ± 10	21 ± 4	13 ± 3

A total number of 60 cells was measured (10 for each morphological and neurochemical type). Statistical comparisons of the mean sizes between the different types of neurons labeled for TH and NADPHd were carried out using an unpaired Student's t-test, with the aid of the SPSS statistical package (SPSS Science, Chicago, IL).

*$P < 0.05$; **$P < 0.01$.

Neurons that contained nNOS also presented a non-pyramidal morphology and were found throughout layers I–VI. However, dendrites were labeled in relatively few cells and therefore more detailed morphological analysis was not performed.

NADPHd-positive neurons were also non-pyramidal and their cell bodies were observed in all the cortical layers as well as underlying the white matter. The intensity of the staining differed in these neurons and was considered as being either moderate (or light) or strong labeling. Moderately labeled neurons were present in all layers, while strongly labeled neurons were mainly localized in the deep cortical layers and the white matter (Fig. 1*B*). The strongly labeled neurons in layers V–VI displayed a variety of forms and sizes (ranging from 127 to 386 μm^2), these NADPHd-positive neurons having larger somata than TH neurons (see Table 1). Morphologically, the most common type of NADPHd-positive neuron was the multipolar cell (Fig. 3*C*,*D*), which constituted 47% of the total population of neurons analyzed (n = 553), followed by the bipolar and bitufted type (23%) and the tripolar type (22%; Fig. 4). Finally, the typical bundles of tight, long, vertically oriented axonal collaterals of double bouquet cells, the short, vertically oriented rows of boutons of chandelier cells axon terminals and the perisomatic terminals originating from basket cells (DeFelipe, 2002) were not stained for TH, nNOS or NADPHd. Thus, the populations of TH-ir, nNOS-ir and NADPHd-positive neurons do not include double bouquet cells, chandelier cells, or basket cells.

TH-ir, nNOS-ir and NADPHd-positive Fibers

Since a detailed morphological description of TH-ir, nNOS-ir and NADPHd-positive fibers has been reported previously (Gaspar *et al.*, 1989; DeFelipe, 1993; Luth *et al.*, 1994), only a brief description will follow. TH-ir fibers were present in all cortical layers, but they were most predominately found in layers I, V and VI (Fig. *1C*,*D*). In layer I, the fibers ran horizontally (Fig. 2*A*,*B*), whereas in the other layers, particularly in layers V–VI, II and the superficial layer III, they were randomly orientated, forming a dense network of thin, beaded axons. As described previously, two main types of TH-ir fibers could be seen (Gaspar *et al.*, 1989): varicose, curvilinear or rectilinear fibers with more or less regularly spaced varicosities and fine fibers showing irregularly spaced oblong swellings. The presence of 'coil-like' accumulations of fibers was occasionally noted in small regions

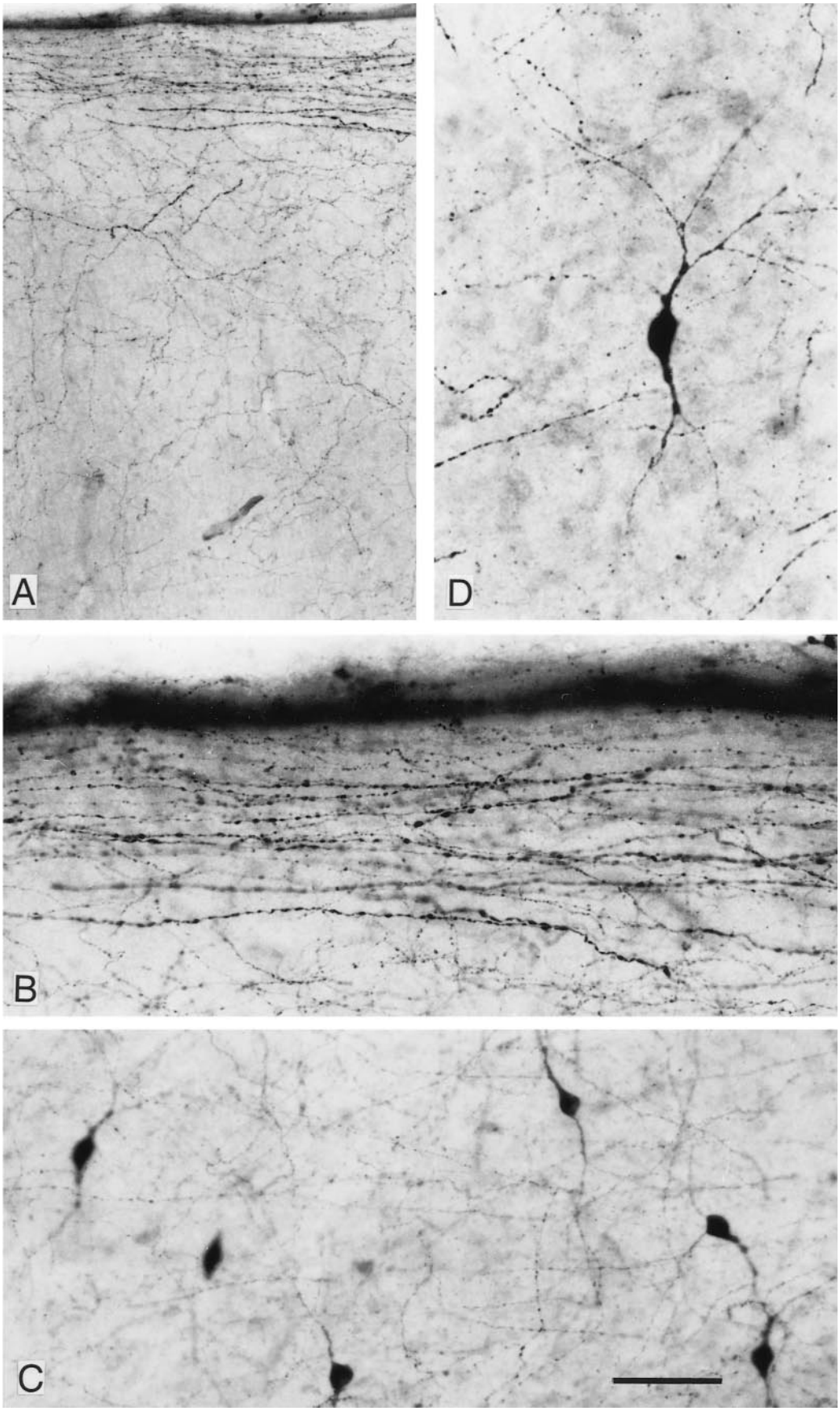

Figure 2. (*A*) Low-power photomicrograph of TH-ir fibers in layers I–III. (*B*) High magnification of TH-ir fibers in layer I, illustrating horizontally oriented fibers. (*C*) Photomicrograph showing TH-ir neurons in layer VI. (*D*) High magnification of a bitufted TH-ir neuron of layer VI. Scale bars = 140 μm (*A*), 35 μm (*B*, *D*) and 70 μm (*C*).

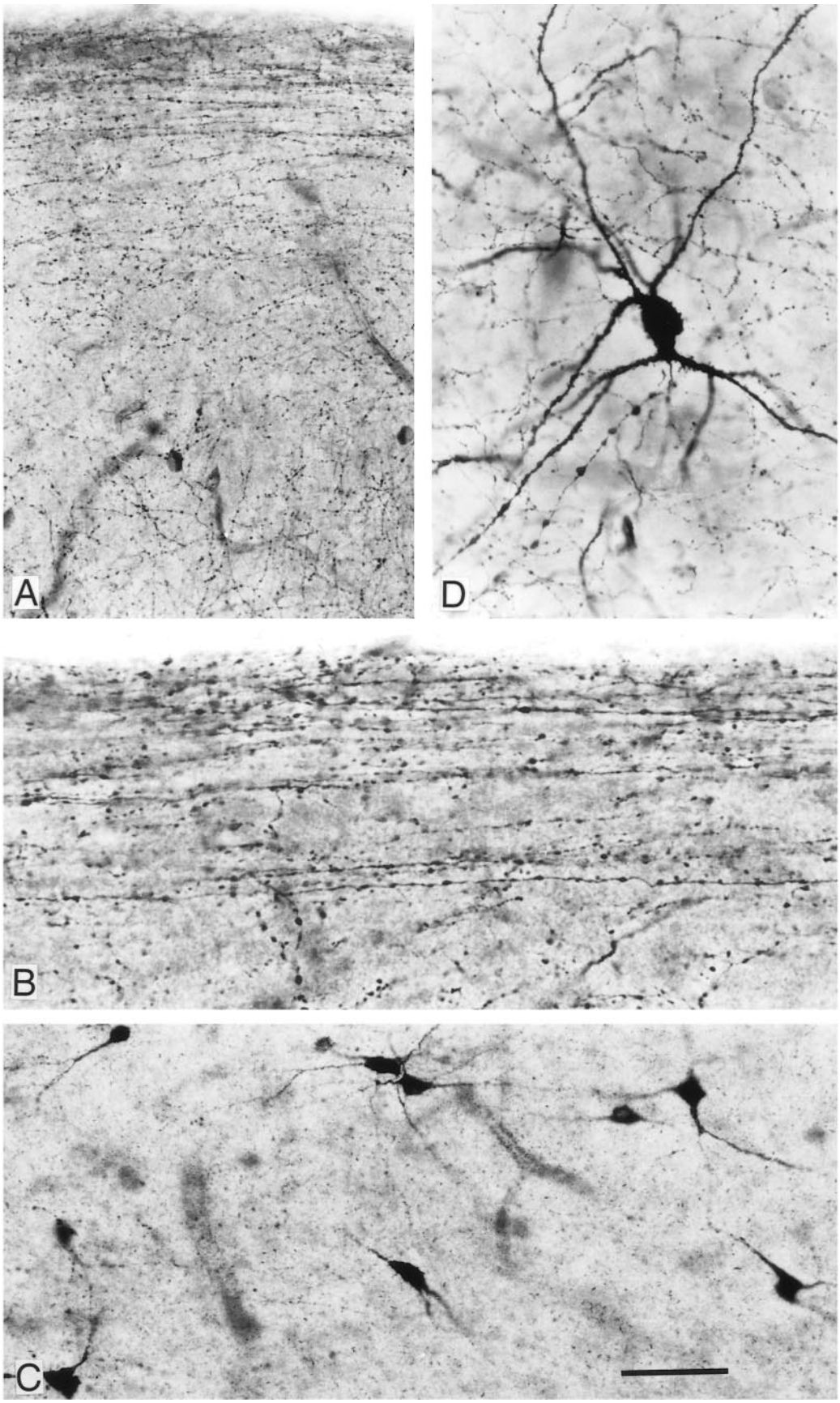

Figure 3. (*A*) Low-power photomicrograph of NADPHd-ir fibers in layers I-III. (*B*) High magnification of NADPHd-ir fibers in layer I, illustrating horizontally oriented fibers. (*C*) High-power photomicrograph showing NADPHd-ir neurons in layer VI. (*D*) High magnification of a multipolar NADPHd-ir neuron of layer VI. Scale bars = 140 μm (*A*), 35 μm (*B*, *D*) and 70 μm (*C*).

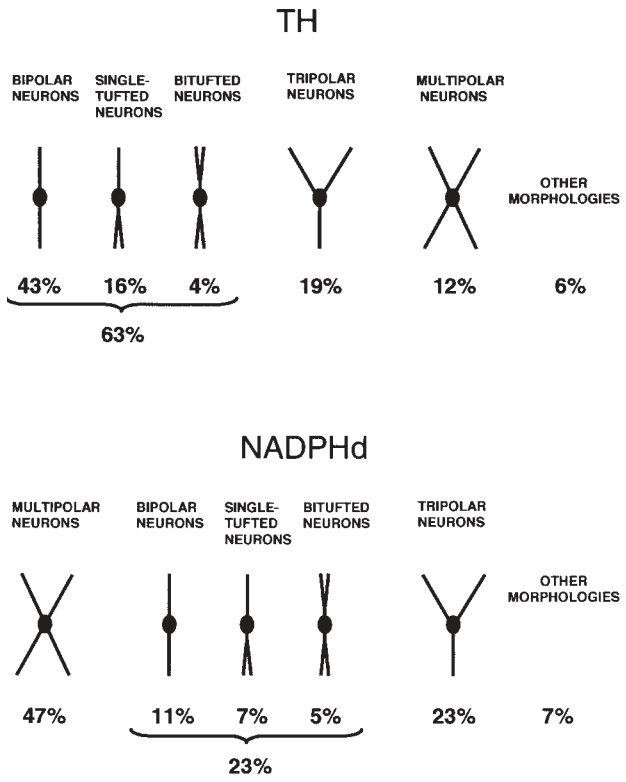

Figure 4. Schematic drawings showing the main morphological types of TH-ir and NADPHd-ir neurons in layers V–VI of the human temporal cortex.

of ~6 μm in layers II–III. Another remarkable feature was the existence of long, ascending axons that extended up from layers V–VI to the superficial layers (Fig. 1*D*). Some of these fibers were clearly seen to originate from TH-ir neurons located in layers V–VI.

Labeling for nNOS in fibers was observed in all layers. In layer I, they were long and preferentially oriented horizontally (Fig. 5*G*). In layers II–VI, the nNOS fibers formed a plexus of thin varicose axons running in all directions. However, the labeling of these fibers was relatively poor and no further morphological analysis was performed.

NADPHd-positive fibers were distributed across all cortical layers. In layer I they formed a plexus of parallel fibers that ran horizontally (Fig. 3*A*,*B*). In layers II–VI, they made up a homogeneous dense network of fibers running in all directions. Most NADPHd-positive fibers in layers II–VI were thin and displayed varicose dilations (boutons; Fig. 3*A*,*D*); however, some fibers were thick, coarsely beaded and strongly stained. A conspicuous feature of this staining was the presence of occasional small accumulations of fibers in all layers except layer I. Some of them appeared to enclose the soma and proximal dendrites of unlabeled neurons and have been called 'basket-like formations' (DeFelipe, 1993). Others were similar to the coil-like accumulations of fibers stained for TH.

Co-localization of TH and nNOS Immunoreactivities in Neuronal Somata and Fibers

As NADPHd-positive neurons in the neocortex have been shown to be the same as those containing the enzyme nNOS (Hope *et al*., 1991; Bredt and Snyder, 1992; Schmidt *et al*., 1992; Vincent and Hope, 1992), nNOS immunocytochemistry was used to study their co-localization with TH immunocytochemistry.

We examined the co-expression of TH and nNOS in the somata of neurons in layers V–VI, where the vast majority of TH neurons were located. The general pattern of immunostaining for TH and nNOS using fluorescent markers was similar to that observed in adjacent sections processed using DAB as the chromogen. However, when immunofluorescent staining was used to detect nNOS, we were able to distinguish two types of neurons: moderately and strongly labeled neurons. The co-localization of TH and nNOS was examined by double labeling sections from the surgically resected cases H39 and H57. The percentages of TH-ir neurons that were also moderately or strongly labeled for nNOS were, respectively, 30 and 2% in H39, and 21 and 1% in H57. Regarding the co-expression of moderate or strong labeling for nNOS with TH, the percentages were, respectively, 42 and 6% in H39, and 20 and 1%, in H57. However, the final estimation was performed considering the two cases together. We found that 25% of the TH-ir neurons were also moderately labeled for nNOS, while 1% of TH-ir neurons were strongly labeled for nNOS. Similarly, 27% of the moderately labeled nNOS neurons co-expressed TH and 3% of the strongly labeled nNOS neurons were also immunoreactive for TH (Fig. 5*A–F*).

The distribution and morphology of TH and NADPHd/nNOS fibers in layer I was apparently similar. However, double labeling of sections failed to revealed fibers in layer I that co-expressed TH and nNOS (Fig. 5*G*). Moreover, in these sections it was apparent that nNOS fibers were mainly located in the upper part of layer I, while TH fibers were mainly distributed in the lower part of this layer (Fig. 5*G*). However, in layers II–VI some fibers that co-expressed both antigens were observed (Fig. 5*H–J*), although a quantitative analysis of these fibers was not performed.

Connections of TH Fibers

As NeuN immunostaining is found only in the soma and proximal dendrites of neurons, double-labeling experiments permitted the examination of the possible connections of TH-ir fibers with NeuN-ir neurons (Fig. 6*A*). To compare the connectivity of TH-ir fibers between layers II and VI, we counted the number of labeled axonal boutons found on the cell bodies of NeuN-ir neurons and in the neuropil in sections double labeled for TH and NeuN (Fig. 6*B*,*C*). Only 6 and 5% of the TH-ir axonal boutons examined (n = 1724) were seen to contact the soma of NeuN-ir neurons in layers II and VI, respectively (Table 2). Thus, most TH-ir axons must form synapses with dendrites. Furthermore, 23 and 32% of NeuN-ir somata (n = 163) in layer II and layer VI, respectively, received at least one TH-ir bouton. The majority of these neurons (~54%) were seen to have one contact, those with two contacts made up 20% of the population and those with three, four or more contacts 5–14% (Table 3). These results suggest that there is a strong preference of TH-ir fibers to connect with dendrites in both layers II and VI. However, only a small, select group of cell bodies received such contacts. In addition, there were no apparent differences in the connections between layer II and VI (Tables 2 and 3).

Discussion

This study has provided us with four major findings. First, all TH-ir cells in the neocortex present a non-pyramidal morphology, although double bouquet cells, chandelier cells and basket cells were not labeled for TH. Secondly, TH is found in at least three different neurochemically defined subpopulations of non-pyramidal neurons in layers V–VI, these neurons being defined by their expression of GABA and nNOS. Thirdly, the

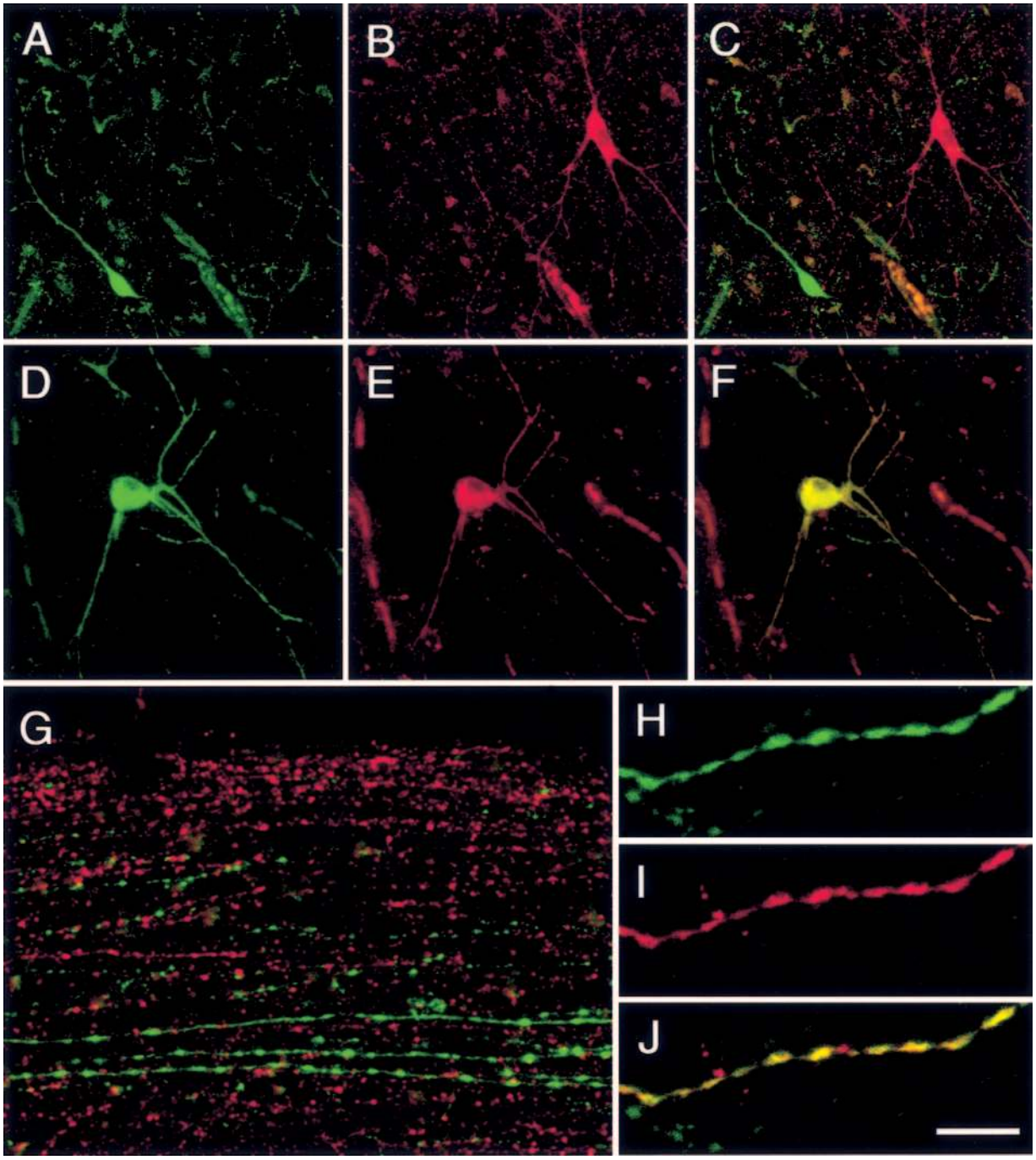

Figure 5. Pseudo-colored confocal images of TH (*A*, *D*, *H*; green) and nNOS (*B*, *E*, *I*; red) immunoreactivity and co-localization of TH with nNOS (*C*, *F*, *G*, *J*). (*A–C*) An example of a TH-ir cell and an nNOS-ir cell that do not co-localize. (*D–F*) A cell that expresses both TH and nNOS. (*G*) TH (green) and nNOS (red) horizontal fibers of layer I. Notice that they do not co-localize. (*H–J*) High-magnification images showing a fiber in deep layers that contains both TH and nNOS. Scale bars = 35 μm (*A–C*), 25 μm (*D–G*) and 7 μm (*H–J*).

prominent plexus in layer I of horizontally oriented fibers that contain TH or nNOS do not co-localize. Fourthly, we found that there is a remarkable preference of TH-ir fibers to connect to dendrites.

What Types of Non-pyramidal Cells are TH-ir Neurons?

The results presented here confirm and extend those obtained in previous studies on TH immunocytochemistry in the human cortex (Gaspar *et al*., 1987; Kosaka *et al*., 1987b; Hornung *et al*., 1989; Kuljis *et al*., 1989). In agreement with these earlier studies, TH immunoreactivity was found in cells that were aspinous, non-pyramidal neurons localized almost exclusively in layers V–VI. Although they showed a variety of shapes and sizes, we found that the most common morphology was that of a bipolar and bitufted form with vertically oriented dendrites (63%). With few exceptions, the different types of non-pyramidal cells can be recognized by the pattern of their axonal arborization (Fairén *et al*., 1984). In this regard, we found that the axons of double bouquet cells, chandelier cells and the classic large basket cells, which constitute three major inhibitory GABAergic inputs to

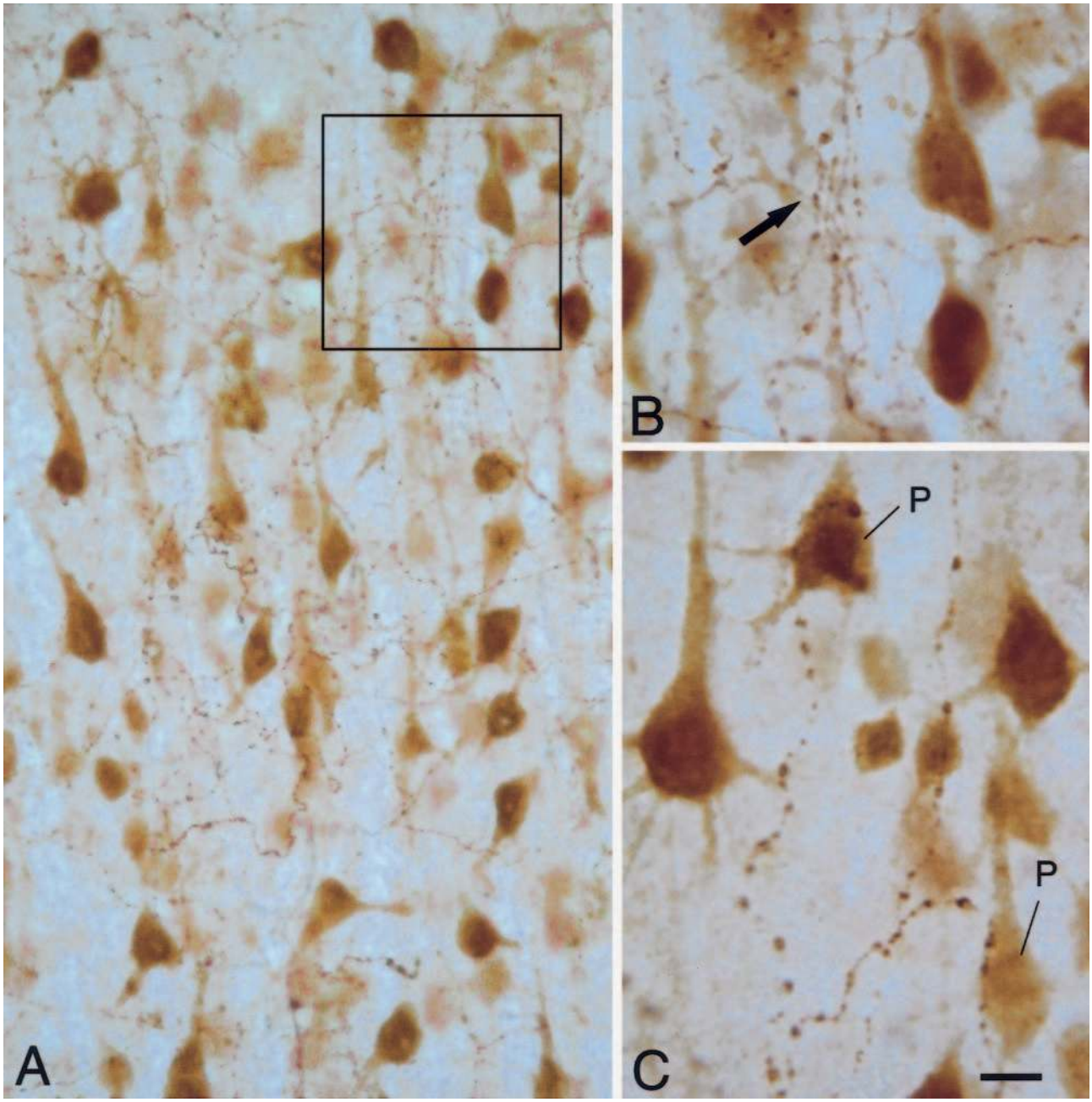

Figure 6. (*A*) Low-power photomicrograph showing double immunocytochemical staining for TH/NeuN. (*B*) High magnification of framed area shown in (*A*). Arrows indicate TH-ir axons distributed in the neuropil. (*C*) High magnification showing NeuN-ir pyramidal cells (P) contacted by TH-ir axonal boutons. Scale bar = 30 μm (*A*) and 10 μm (*B, C*).

pyramidal cells in the primate neocortex (DeFelipe, 2002), did not contain TH. Since TH-ir, vertically-oriented, ascending axons were also commonly found and some of these axons were seen to arise from TH-ir neurons, it is possible that Martinotti cells or cells with an ascending axon are among the population of TH-ir neurons. Further studies will be necessary to find out exactly which groups of non-pyramidal neurons express TH.

Neurochemical Profiles of TH-ir Neurons

We found that ~26% of TH neurons co-expressed nNOS. The group of neurons that contained both TH and nNOS or TH only can be further characterized neurochemically on the basis of data derived from earlier immunocytochemical studies performed on the same brain material. For instance, nitrergic neurons have been chemically defined as a subpopulation of GABAergic cells that contain the peptides somatostatin and neuropeptide Y, and that frequently contain the calcium-binding protein calbindin. These nitrergic neurons do not contain parvalbumin and calretinin and show little or no co-localization with the other peptides (González-Albo *et al.*, 2001). Thus, it seems likely that TH–nNOS-ir neurons also express GABA and contain calbindin, somatostatin and neuropeptide Y, but not other calcium-binding proteins or peptides. Additionally, it has been reported that in the human neocortex only 50% of TH-ir neurons contain GABA (Trottier *et al.*, 1989). As TH-ir neurons that express nNOS contain GABA, it is likely that those lacking nNOS (74%) include the population that also lacks GABA. In conclusion, based on their GABA and nNOS content, TH-ir

Table 2

Percentage of cell bodies labeled for NeuN contacted by TH-ir axonal boutons, percentage of TH-ir axonal boutons in apposition with the somata of NeuN-ir neurons and percentage of TH-ir axonal boutons found in the neuropil

Cortical layers	Percentage of TH-ir axonal boutons in apposition with the somata of NeuN-ir neurons	Percentage of TH-ir axonal boutons in the neuropil	Percentage of NeuN-ir neurons contacted by TH-ir axonal boutons
II	6 (6, 6 and 7)	94 (94, 94 and 93)	23 (23, 26 and 19)
VI	5 (6, 5 and 8)	95 (94, 95 and 92)	32 (36, 29 and 22)

The values found per individual case (H39, H57 and H59, respectively) are shown in parentheses.

Table 3

Percentage of cell bodies stained for NeuN contacted by 1, 2, 3, 4 and 5 or more TH-ir axonal boutons

Cortical layers	One TH-ir bouton	Two TH-ir boutons	Three TH-ir boutons	Four TH-ir boutons	Five or more TH-ir boutons
Percentage of NeuN-ir neurons in layer II	52	19	5	14	10
Percentage of NeuN-ir neurons in layer VI	56	22	9	4	9

neurons are made up of at least three subpopulations of non-pyramidal cells in the human temporal cortex: TH–nNOS-GABA-positive, TH–GABA-positive/nNOS-negative and TH-positive/GABA–nNOS-negative.

Origin, Distribution and Neurochemical Profiles of TH Fibers in Layer I

The data that we present here confirm that in the cerebral cortex, TH fibers originate from intrinsic and extrinsic sources, i.e. that these fibers are from non-pyramidal cells of layers V and VI and from the major catecholaminergic cell groups of the upper brainstem, respectively (Hokfelt *et al.*, 1976, 1977; Lindvall *et al.*, 1983; Gaspar *et al.*, 1987; Kosaka *et al.*, 1987b; Hornung *et al.*, 1989; Kuljis *et al.*, 1989; Kostal *et al.*, 1999). None of the major cortical afferent systems (thalamocortical, associational and commissural), nor any adult cortical neurons give rise to such long, horizontally oriented fibers in layer I as those labeled for TH, NADPHd and nNOS. Thus, it seems most probable that these fibers arise from subcortical, extra-thalamic nuclei (DeFelipe, 1993). Furthermore, these layer-I fibers are similar to those labeled for dopamine, noradrenaline or serotonin (Morrison and Magistretti, 1983; Morrison *et al.*, 1984; Fallon and Loughlin, 1987). In the present study, we found that the TH- and nNOS-ir fibers in layer I shared a similar morphology, but no double-labeled fibers were observed. Moreover, it was evident that the two types of fibers run at different levels within layer I. In conclusion, the TH afferent system of layer I of the human temporal cortex does not contain nitric oxide, each group of fibers is clearly segregated.

Connectivity of TH-ir Axon Terminals

In the cerebral cortex, TH-ir axon terminals have been shown to establish symmetrical synapses with the dendritic shafts of both pyramidal and non-pyramidal cells, and with the dendritic spines of pyramidal cells (Cowan *et al.*, 1994; Sesack *et al.*, 1995b, 1998; Carr and Sesack, 1996; Carr *et al.*, 1999; Erickson *et al.*, 2000). However, these electron microscopy studies are based on the analysis of relatively few TH-ir axon terminals, a limitation when trying to establish general observations regarding circuitry. For this reason, the examination of sections double labeled for TH and other markers to visualize possible axon targets is a useful complementary method for the study of cortical circuits. Since a large number of TH-ir axon terminals can be readily examined in this way, it is more feasible to establish whether particular targets, such as somata or dendrites, or specific neurons, are innervated or not. For example, a quantitative analysis in the monkey prefrontal cortex combining immunostaining for TH and intracellular injections with Lucifer Yellow revealed the widespread innervation of both pyramidal and non-pyramidal cell dendritic arborizations by TH-ir axons (Krimer *et al.*, 1997). In addition, these authors also found a higher density of TH appositions on the spiny dendritic arborization of pyramidal cells in layer II and superficial layer III as compared with pyramidal cells of deep layer III and layers V–VI. Furthermore, it has been shown that in the monkey prefrontal cortex, TH-ir axon terminals innervate GABAergic non-pyramidal cells expressing parvalbumin but not calretinin (Sesack *et al.*, 1995a, 1998). Additionally, a marked heterogeneity in the density of TH-ir fibers has been demonstrated among different cortical areas and layers of the monkey neocortex (Lewis *et al.*, 1987). Thus, previous studies have established that catecholaminergic innervation of both pyramidal and non-pyramidal cells occurs and that this is selective for area, laminar and neuronal cell types.

In this study we have found that the number of TH-ir terminals in contact with somata was remarkably low (6%) compared to those found on the neuropil (94%). Since TH-ir axon terminals arise from both intrinsic cortical neurons and from subcortical nuclei, the precise connections of these cortical neurons could not be established here. For example, we cannot discard the possibility that these neurons were a source of TH-ir axo-somatic contacts in both layers (in layer VI through local axons and in the upper layers through their vertical connections).

Functional Implications

It has been established that in the monkey neocortex, TH-ir axons innervate mainly dendritic processes and that certain populations of pyramidal cells are more densely innervated by TH-ir axons than others. Moreover, not all non-pyramidal cells are targets of these axons. Taken together, these data indicate that cortical circuits in which TH axons are involved are complex but highly selective. It will be necessary further to unravel these circuits in order to understand better the role of TH in cortical function. Furthermore, the catecholaminergic end product of cortical TH-ir neurons is unknown. Previous immunocytochemical studies have shown that cortical TH neurons do not express aromatic amino acid decarboxylase and dopamine-β-hydroxylase (Gaspar *et al.*, 1987; Ikemoto *et al.*, 1999), the enzymes which are necessary for the synthesis of dopamine and noradrenaline, respectively. However, while these studies suggest that these cortical TH neurons only synthesize dopa, it cannot be excluded that the levels of one or both of these enzymes in these cells may be below the sensitivity of the currently available immunocytochemical procedures. Alternatively, TH, although present, might be inactive in cortical neurons. Therefore, further studies are necessary to obtain a better idea about the functional role that TH-ir neurons and fibers play in cortical circuitry.

Finally, neurons or neuronal processes containing nNOS or catecholamines have been shown to be in close proximity to intraparenchymal microvessels (Raichle *et al.*, 1975; Cohen *et al.*, 1995; Estrada and DeFelipe, 1998; Krimer *et al.*, 1998).

As a result, it is tempting to suggest that both catecholamines and nitric oxide might directly act on the regulation of cortical microcirculation. Therefore, it is possible that TH/nNOS neurons (or a subpopulation of them) are involved in the coupling between local cortical blood flow and synaptic activity by a mechanism other than that employed by those neurons that contain only nNOS.

In summary, TH-ir neurons constitute a subpopulation of non-pyramidal cells in layers V–VI that are morphologically and neurochemically heterogeneous. The vast majority of TH-ir axons (94%) were found in the neuropil, although the connections of cortical TH-ir neurons could not be established. However, based on the morphological characteristics and patterns of axonal arborization of TH-ir axons, we conclude that the population of TH-ir neurons does not include double bouquet cells, chandelier cells or large basket cells, but probably does include Martinotti cells. Furthermore, the conclusions drawn from the co-localization of TH and nNOS in neuronal somata and fibers indicate that the partial overlapping of the catecholaminergic and nitrergic systems is likely to be due to the cortical intrinsic neurons expressing both TH and nNOS.

Notes

This work was supported by grants awarded to J.D.F. from the Spanish Ministry of Science and Technology (DGCYT PM99-0105) and the 'Comunidad de Madrid' (08.5/0027/2001.1). R.B.-P. is supported by a fellowship from the 'Comunidad de Madrid' (01/0782/2000). We thank A. Ortiz for technical help and C. Hernández for assistance with the confocal microscopy.

Address correspondence to Dr Javier DeFelipe, Instituto Cajal (CSIC), Avenida Dr Arce 37, 28002 Madrid, Spain. Email: defelipe@cajal.csic.es.

References

Akbarian S, Bunney WE Jr, Potkin SG, Wigal SB, Hagman JO, Sandman CA, Jones EG (1993) Altered distribution of nicotinamide-adenine dinucleotide phosphate-diaphorase cells in frontal lobe of schizophrenics implies disturbances of cortical development. Arch Gen Psychiatry 50:169–177.

Bertini G, Peng ZC, Bentivoglio M (1996) The chemical heterogeneity of cortical interneurons: nitric oxide synthase vs. calbindin and parvalbumin immunoreactivity in the rat. Brain Res Bull 39:261–266.

Bredt DS, Snyder SH (1992) Nitric oxide, a novel neuronal messenger. Neuron 8:3–11.

Bredt DS, Glatt CE, Hwang PM, Fotuhi M, Dawson TM, Snyder SH (1991) Nitric oxide synthase protein and mRNA are discretely localized in neuronal populations of the mammalian CNS together with NADPH diaphorase. Neuron 7:615–624.

Carr DB, Sesack SR (1996) Hippocampal afferents to the rat prefrontal cortex: synaptic targets and relation to dopamine terminals. J Comp Neurol 369:1–15.

Carr DB, O'Donnell P, Card JP, Sesack SR (1999) Dopamine terminals in the rat prefrontal cortex synapse on pyramidal cells that project to the nucleus accumbens. J Neurosci 19:11049–11060.

Cohen Z, Ehret M, Maitre M, Hamel E (1995) Ultrastructural analysis of tryptophan hydroxylase immunoreactive nerve terminals in the rat cerebral cortex and hippocampus: their associations with local blood vessels. Neuroscience 66:555–569.

Cowan RL, Sesack SR, Van Bockstaele EJ, Branchereau P, Chain J, Pickel VM (1994) Analysis of synaptic inputs and targets of physiologically characterized neurons in rat frontal cortex: combined *in vivo* intracellular recording and immunolabeling. Synapse 17:101–114.

Dawson TM, Bredt DS, Fotuhi M, Hwang PM, Snyder SH (1991) Nitric oxide synthase and neuronal NADPH diaphorase are identical in brain and peripheral tissues. Proc Natl Acad Sci USA 88:7797–7801.

DeFelipe J (1993) A study of NADPH diaphorase-positive axonal plexuses in the human temporal cortex. Brain Res 615:342–346.

DeFelipe J (2002) Cortical interneurons: from Cajal to 2001. Prog Brain Res 136:215–238.

Erickson SL, Sesack SR, Lewis DA (2000) Dopamine innervation of monkey entorhinal cortex: postsynaptic targets of tyrosine hydroxylase-immunoreactive terminals. Synapse 36:47–56.

Estrada C, DeFelipe J (1998) Nitric oxide-producing neurons in the neocortex: morphological and functional relationship with intraparenchymal microvasculature. Cereb Cortex 8:193–203.

Fairén A, DeFelipe J, Regidor J (1984) Non pyramidal neurons. General account. In: Cerebral cortex: cellular components of the cerebral cortex (Peters A, Jones EG, eds), pp. 201–253. New York: Plenum Press.

Fallon JH, Loughlin SE (1987) Monoamine innervation of the cerebral cortex and a theory of the role of monoamines in cerebral cortex and basal ganglia. In: Cerebral cortex: further aspects of cortical function including hippocampus (Jones EG, Peters A, eds), pp. 41–127. New York: Plenum Press.

Garey LJ (1994) Brodmann's localisation in the cerebral cortex. London: Smith-Gordon.

Gaspar P, Berger B, Febvret A, Vigny A, Krieger-Poulet M, Borri-Voltattorni C (1987) Tyrosine hydroxylase-immunoreactive neurons in the human cerebral cortex: a novel catecholaminergic group? Neurosci Lett 80:257–262.

Gaspar P, Berger B, Febvret A, Vigny A, Henry JP (1989) Catecholamine innervation of the human cerebral cortex as revealed by comparative immunohistochemistry of tyrosine hydroxylase and dopamine-beta-hydroxylase. J Comp Neurol 279:249–271.

Goldman-Rakic PS (1998) The cortical dopamine system: role in memory and cognition. Adv Pharmacol 42:707–11.

Gonchar Y, Burkhalter A (1997) Three distinct families of GABAergic neurons in rat visual cortex. Cereb Cortex 7:347–358.

González-Albo MC, Gómez-Utrero E, Sánchez A, Sola RG, DeFelipe J (2001) Changes in the colocalization of glutamate ionotropic receptor subunits in the human epileptic temporal lobe cortex. Exp Brain Res 138:398–402.

Hashikawa T, Leggio MG, Hattori R, Yui Y (1994) Nitric oxide synthase immunoreactivity colocalized with NADPH-diaphorase histochemistry in monkey cerebral cortex. Brain Res 641:341–349.

Hof PR, Glezer II, Revishchin AV, Bouras C, Charnay Y, Morgane PJ (1995) Distribution of dopaminergic fibers and neurons in visual and auditory cortices of the harbor porpoise and pilot whale. Brain Res Bull 36:275–284.

Hökfelt T, Johansson O, Fuxe K, Goldstein M, Park D (1976) Immunohistochemical studies on the localization and distribution of monoamine neuron systems in the rat brain. I. Tyrosine hydroxylase in the mesencephalon and diencephalon. Med Biol 54:427–453.

Hökfelt T, Johansson O, Fuxe K, Goldstein M, Park D (1977) Immunohistochemical studies on the localization and distribution of monoamine neuron systems in the rat brain. II. Tyrosine hydroxylase in the telencephalon. Med Biol 55:21–40.

Hope BT, Vincent SR (1989) Histochemical characterization of neuronal NADPH-diaphorase. J Histochem Cytochem 37:653–661.

Hope BT, Michael GJ, Knigge KM, Vincent SR (1991) Neuronal NADPH diaphorase is a nitric oxide synthase. Proc Natl Acad Sci USA 88:2811–2814.

Hornung JP, Tork I, De Tribolet N (1989) Morphology of tyrosine hydroxylase-immunoreactive neurons in the human cerebral cortex. Exp Brain Res 76:12–20.

Houser CR, Vaughn JE, Hendry SHC, Jones EG, Peters A (1984) GABA neurons in the cerebral cortex. In: Cerebral cortex, vol. 2. Functional properties of cortical cells (Jones EG, Peters A, eds), pp. 63–89. New York: Plenum Press.

Huang PL, Dawson TM, Bredt DS, Snyder SH, Fishman MC (1993) Targeted disruption of the neuronal nitric oxide synthase gene. Cell 75:1273–1286.

Ikemoto K, Kitahama K, Nishimura A, Jouvet A, Nishi K, Arai R, Jouvet M, Nagatsu I (1999) Tyrosine hydroxylase and aromatic L-amino acid decarboxylase do not coexist in neurons in the human anterior cingulate cortex. Neurosci Lett 269:37–40.

Kosaka T, Kosaka K, Hataguchi Y, Nagatsu I, Wu JY, Ottersen OP, Storm-Mathisen J, Hama K (1987a) Catecholaminergic neurons containing GABA-like and/or glutamic acid decarboxylase-like immunoreactivities in various brain regions of the rat. Exp Brain Res 66:191–210.

Kosaka T, Hama K, Nagatsu I (1987b) Tyrosine hydroxylase-immunoreactive intrinsic neurons in the rat cerebral cortex. Exp Brain Res 68:393–405.

Kostal L, Vyboh P, Savory CJ, Jurani M, Kubikova L, Blazicek P (1999)

Influence of food restriction on dopamine receptor densities, catecholamine concentrations and dopamine turnover in chicken brain. Neuroscience 94:323–328.
Krimer LS, Jakab RL, Goldman-Rakic PS (1997) Quantitative three-dimensional analysis of the catecholaminergic innervation of identified neurons in the macaque prefrontal cortex. J Neurosci 17:7450–7461.
Krimer LS, Muly EC, Williams GV, Goldman-Rakic PS (1998) Dopaminergic regulation of cerebral cortical microcirculation. Nat Neurosci 1:286–289.
Kubota Y, Hattori R, Yui Y (1994) Three distinct subpopulations of GABAergic neurons in rat frontal agranular cortex. Brain Res 649:159–173.
Kuljis RO, Martin-Vasallo P, Peress NS (1989) Lewy bodies in tyrosine hydroxylase-synthesizing neurons of the human cerebral cortex. Neurosci Lett 106:49–54.
Lewis DA, Lieberman JA (2000) Catching up on schizophrenia: natural history and neurobiology. Neuron 28:325–334.
Lewis DA, Campbell MJ, Foote SL, Goldstein M, Morrison JH (1987) The distribution of tyrosine hydroxylase-immunoreactive fibers in primate neocortex is widespread but regionally specific. J Neurosci 7:279–290.
Lidow MS, Williams GV, Goldman-Rakic PS (1998) The cerebral cortex: a case for a common site of action of antipsychotics. Trends Pharmacol Sci 19:136–40.
Lindvall O, Bjorklund A, Skagerberg G (1983) Dopamine-containing neurons in the spinal cord: anatomy and some functional aspects. Ann Neurol 14:255–260.
Lüth HJ, Hedlich A, Hilbig H, Winkelmann E, Mayer BJ (1994) Morphological analyses of NADPH-diaphorase/nitric oxide synthase positive structures in human visual cortex. J Neurocytol 23:770–782.
Morrison JH, Magistretti PJ (1983) Monoamines and peptides in cerebral cortex. Contrasting principles of cortical organization. Trends Neurosci 6:146–151.
Morrison JH, Foote SL, Bloom FE (1984) Regional, laminar, developmental and functional characteristics of noradrenaline and serotonin innervation patterns in monkey cortex. In: Monoamine innervation of the cerebral cortex (Descarries L, Reader TR, Jasper HH, eds), pp. 61–75. New York: Alan R. Liss.
Mullen RJ, Buck CR, Smith AM (1992) NeuN, a neuronal specific nuclear protein in vertebrates. Development 116:201–211.
Palmer AM (1996) Neurochemical studies of Alzheimer's disease. Neurodegeneration 5:381–91.
Raichle ME, Hartman BK, Eichling JO, Sharpe LG (1975) Central noradrenergic regulation of cerebral blood flow and vascular permeability. Proc Natl Acad Sci USA 72:3726–3730.
Sarnat HB, Nochlin D, Born DE (1998) Neuronal nuclear antigen (NeuN): a marker of neuronal maturation in early human fetal nervous system. Brain Dev 20:88–94.
Schmidt HH, Gagne GD, Nakane M, Pollock JS, Miller MF, Murad F (1992) Mapping of neural nitric oxide synthase in the rat suggests frequent co- localization with NADPH diaphorase but not with soluble guanylyl cyclase, and novel paraneural functions for nitrinergic signal transduction. J Histochem Cytochem 40:1439–1456.
Sesack SR, Bressler CN, Lewis DA (1995a) Ultrastructural associations between dopamine terminals and local circuit neurons in the monkey prefrontal cortex: a study of calretinin-immunoreactive cells. Neurosci Lett 200:9–12.
Sesack SR, Snyder CL, Lewis DA (1995b) Axon terminals immunolabeled for dopamine or tyrosine hydroxylase synapse on GABA-immunoreactive dendrites in rat and monkey cortex. J Comp Neurol 363:264–280.
Sesack SR, Hawrylak VA, Melchitzky DS, Lewis DA (1998) Dopamine innervation of a subclass of local circuit neurons in monkey prefrontal cortex: ultrastructural analysis of tyrosine hydroxylase and parvalbumin immunoreactive structures. Cereb Cortex 8:614–622.
Smeets WJ, González A (2000) Catecholamine systems in the brain of vertebrates: new perspectives through a comparative approach. Brain Res Rev 33:308–379.
Trottier S, Geffard M, Evrard B (1989) Co-localization of tyrosine hydroxylase and GABA immunoreactivities in human cortical neurons. Neurosci Lett 106:76–82.
Unger JW, Lange W (1992) NADPH-diaphorase-positive cell populations in the human amygdala and temporal cortex: neuroanatomy, peptidergic characteristics and aspects of aging and Alzheimer's disease. Acta Neuropathol (Berl) 83:636–646.
Valtschanoff JG, Weinberg RJ, Kharazia VN, Schmidt HH, Nakane M, Rustioni A (1993) Neurons in rat cerebral cortex that synthesize nitric oxide: NADPH diaphorase histochemistry, NOS immunocytochemistry, and colocalization with GABA. Neurosci Lett 157:157–161.
Vincent SR, Hope BT (1992) Neurons that say NO. Trends Neurosci 15:108–113.
Wolf HK, Buslei R, Schmidt-Kastner R, Schmidt-Kastner PK, Pietsch T, Wiestler OD, Bluhmke I (1996) NeuN: a useful neuronal marker for diagnostic histopathology. J Histochem Cytochem 44:1167–1171.
Yan XX, Jen LS, Garey LJ (1996) NADPH-diaphorase-positive neurons in primate cerebral cortex colocalize with GABA and calcium-binding proteins. Cereb Cortex 6:524–529.